Frontiers in Bioscience Landmark

Front. Biosci. (Landmark Ed) **2025**; 30(3): 25361
https://doi.org/10.31083/FBL25361

Original Research

NOL6 Promotes Tumor Progression by Facilitating Cancer Cell-Induced Platelet Aggregation and Angiogenesis in Breast Cancer

Tingting Zhang[1], Cheng Lu[2,*], Mingming Lv[2], Shengwang Du[1], Xinjun Wu[1]

[1]Department of General Surgery, Lianyungang Affiliated Hospital of Nanjing University of Traditional Chinese Medicine, 222000 Lianyungang, Jiangsu, China
[2]Department of Breast, Nanjing Maternal and Child Health Hospital, 210094 Nanjing, Jiangsu, China
*Correspondence: 20195080@njucm.edu.cn (Cheng Lu)

Academic Editor: Amancio Carnero Moya
Submitted: 24 June 2024 Revised: 15 October 2024 Accepted: 22 October 2024 Published: 21 March 2025

Abstract

Background: Breast cancer (BC) is a prevalent malignancy among women, and numerous investigations have reported that platelet aggregation may play a role in BC progression. Thus, identifying new targets for BC is essential. In this regard, we focused on nucleolar protein 6 (NOL6), located on chromosome *9p13*, which is implicated in tumor development. **Objective**: To investigate NOL6 expression in BC, examine its role in platelet aggregation and angiogenesis, and elucidate the underlying mechanisms. **Methods**: Bioinformatic analyses, immunoblotting, and quantitative real-time polymerase chain reaction (qPCR) were performed to assess NOL6 expression in BC. Cell counting kit-8 (CCK-8) and 5-ethynyl-2′-deoxyuridine (EdU) assays were conducted to determine the impact of NOL6 on BC cell proliferation. Immunostaining, enzyme-linked immunosorbent assay (ELISA), and flow cytometry (FCM) assays were utilized to analyze the effects of NOL6 on platelet aggregation. Tube formation and transwell assays were performed to examine angiogenesis and invasion, immunoblot assays were used to confirm the underlying mechanisms, and tumor growth assays in mice were conducted to validate the findings *in vivo*. **Results**: NOL6 was found to be highly expressed in BC and was associated with patient prognosis, platelet aggregation, and angiogenesis. Its knockdown inhibited BC cell proliferation and reduced platelet aggregation induced by BC cells. Additionally, NOL6 depletion impaired angiogenesis and migration of BC cells. *In vivo* studies confirmed that NOL6 promotes tumor growth. Mechanistically, NOL6 enhances the Twisted spiral transcription factor 1 (Twist1)/galectin-3 axis, contributing to BC progression. **Conclusions**: NOL6 can promote tumor progression by facilitating platelet aggregation and angiogenesis in BC cells through the Twist1/galectin-3 axis.

Keywords: breast cancer (BC); Nucleolar Protein 6 (NOL6); platelet aggregation; angiogenesis; Twist1/galectin-3

1. Introduction

Breast cancer (BC) is a prevalent malignancy among women worldwide, and although advances in its early detection have led to a decline in mortality rates, metastasis remains the leading cause of death among BC, accounting for over 90% of cancer-related fatalities [1]. Despite extensive research into deciphering its metastatic intricacies, the precise mechanisms are still not fully understood. Recently, platelet activation has emerged as a potential therapeutic target for BC [2], as inhibiting platelet function has been shown to suppress metastasis [3]. Although current literature suggests that platelet aggregation plays a significant role in BC progression [4], the mechanisms through which tumor cells instruct platelets to contribute to metastasis are not yet clear.

Nucleolar Protein 6 (NOL6) is a nucleolar protein located on chromosome *9p13* with a total length of 11434 bp [5]. It is mainly localized in the nucleolus of cells and plays a significant role in tumor biology. NOL6 is aberrantly overexpressed in prostate cancer, where it promotes cell proliferation and inhibits apoptosis [6]. In gastric cancer, NOL6 overexpression enhances cell viability and reduces apoptosis [6,7]. Additionally, NOL6 supports endometrial cancer cell growth by regulating Twisted spiral transcription factor 1 (Twist1) expression [8]. Despite these findings, the role of NOL6 in BC remains unexplored, and its mechanisms are not well understood.

Analysis of The Cancer Genome Atlas (TCGA) data indicates that NOL6 is highly expressed in BC patients, with elevated levels correlating with poor prognosis [8]. NOL6 has been shown to upregulate TWIST1, which promotes the malignant phenotype of BC cells by enhancing their motility [7]. Furthermore, TWIST1 increases the expression of galectin-3 [4,9]. Galectin-3, an anti-receptor for Glycoprotein VI (GPVI) on BC cells, facilitates platelet adhesion and aggregation, contributing to tumor progression [10,11]. Despite these associations, the exact role of NOL6 in BC progression remains unclear.

In this study, we investigated the role of NOL6 in BC and found that NOL6 promoted the Twist1/galectin-3 axis, thereby facilitating platelet aggregation and angiogenesis in BC cells, which may contribute to the malignant phenotype of the disease. Thus, we propose NOL6 as a novel therapeutic target for BC.

Table 1. Characteristics of the study populations.

	Cancer patients	Healthy subjects	*p* value	z value	t value
Female, no. (%)	40 (100%)	20 (100%)	/		
Age, years Median (IQR)	60.00 (22.50)	58.00 (14.50)	0.236	1.185	
Stage, no. (%)			/		
I	5 (12.5)				
II	13 (32.5)				
III	7 (17.5)				
Metastasis	15 (37.5)				
Tumor size, no. (%)			/		
<2 cm	10 (25)				
2–5 cm	27 (67.5)				
>5 cm	3 (7.5)				
P-selectin, ng 10^{-8}/cell Median (IQR)	66.50 (24.00)	46.50 (8.50)	<0.001	5.915	
Blood coagulation function					
Prothrombin time (PT), s Median (IQR)	8.35 (1.05)	15.20 (1.35)	<0.001	6.263	
Activated partial thromboplastin time (APTT), s Median (IQR)	29.60 (2.83)	43.25 (3.90)	<0.001	6.275	
Fibrinogen (FIB), g/L Median (IQR)	6.70 (1.73)	3.50 (0.28)	<0.001	6.285	
D-D, µg/L Mean ± sd	876.28 ± 43.87	331.00 ± 44.52	<0.001		45.162
Indicators of Angiogenesis					
VEGF, ng 10^{-8}/cell Median (IQR)	102.00 (23.00)	51.00 (12.50)	<0.001	6.196	
Ang-1, ng 10^{-8}/cell Median (IQR)	31.00 (6.75)	20.50 (9.00)	<0.001	5.063	

IQR, Interquartile range; VEGF, vascular endothelial growth factor.

2. Materials and Methods

2.1 Bioinformatic Analysis

The expression of NOL6 in breast cancer tissues was analyzed using the TCGA database (https://portal.gdc.cancer.gov/) and prognostic analysis was conducted using the Gene Expression Profiling Interactive Analysis (GEPIA) tool (http://gepia.cancer-pku.cn/).

2.2 Samples

This study was conducted in accordance with the principles outlined in the Declaration of Helsinki. The serum samples were collected from 40 BC patients and 20 healthy controls at Lianyungang Affiliated Hospital of Nanjing University of Traditional Chinese Medicine. This study was approved by our hospital's Ethics Committee. The informed consent has been obtained by the patients or their families/legal guardians. Peripheral blood was processed using Ficoll lymphocyte isolation solution, and the clinical and pathological characteristics of the BC patients and healthy controls were assessed (Table 1).

2.3 Cell Culture and Transfection

BC cell lines, including MCF-7 (SCSP-531), MDA-MB-231 (TCHu227), as well as the normal breast cell line HMEC (GNHu46), were purchased from Cell Bank, Chinese Academy of Sciences (Shanghai, China). SW527 (5922-60-1) was bought from ATCC (Manassas, VA, USA). They were maintained in Dulbecco's Modified Eagle Medium (DMEM; Gibco, Carlsbad, CA, USA, Cat# 11965092, Lot# 2123456) supplemented with 10% fetal bovine serum (FBS; Gibco, Cat# 10099141, Lot# 3456789) and incubated at 37 °C in a 5% CO_2 atmosphere. All cell lines were authenticated by short tandem repeats (STR) profiling and tested negative for mycoplasma. *NOL6* shRNA plasmids were constructed in our lab. For gene knockdown or overexpression, plasmid containing DNA (pcDNA) plasmids or shRNA constructs targeting *NOL6* (5′-CTGACCCTGGGACTCCTTC-3′), and negative control (sh-NC) (5′-GCAGGAATTGGAACATTAT-3′) were transfected into MCF-7 cells using Lipofectamine 2000 (Invitrogen, Shanghai, China). Transfection efficiency was assessed by quantitative real-time polymerase chain reaction (qPCR) and immunoblotting 48 hours post-transfection.

2.4 Immunoblot Assay

The cell samples were lysed using RIPA buffer (Beyotime, Beijng, China). Protein concentration was assessed using a Bovine serum albumin (BCA) protein assay kit (Thermo Fisher Scientific, Waltham, MA, USA). Equal amounts of protein (30 µg) were separated by 10% SDS-PAGE and transferred to PVDF membranes (Millipore, Burlington, MA, USA). Membranes were blocked with 5% dry milk and incubated with primary antibodies against Nucleolar Protein 6 (NOL6) (Abcam, Cambridge, UK, ab228836; 1:500), Twist1 (Abcam, ab50887; 1:1000), galectin-3 (Abcam, ab76245; 1:500), platelet-derived growth factor (PDGF) (Abcam, ab178439; 1:1000), Vascular endothelial growth factor (VEGF) (Abcam, ab291246; 1:500), and beta-actin (Abcam, ab8226; 1:3000). After incubation with Horseradish peroxidase (HRP)-conjugated secondary antibodies (Goat Anti-Rabbit antibody, Abcam, ab6721; 1:2000), the protein bands were visualized using the enhanced chemiluminescence (ECL) detection system (RPN2106, GE, Marlborough, MA, USA).

2.5 Quantitative PCR

RNA was extracted from tissue and cell samples using Trizol reagent (TaKaRa, Kusatsu City, Japan), RNA concentration and purity were assessed using a NanoDrop spectrophotometer (Thermo Fisher Scientific, USA), total RNA was reverse transcribed into cDNA using the RT reagent Kit (Takara), and quantitative PCR was performed using SYBR Ex Taq™ II (Takara). The primer sequences used were: *NOL6*: Forward: 5′-AGGAAGCGTACATTGGCTGAA-3′, Reverse: 5′-GTCTCCCGAAGGCGATTAAGC-3′; *TWIST1*: Forward: 5′-GTCCGCAGTCTTACGAGGAG-3′, Reverse: 5′-GCTTGAGGGTCTGAATCTTGCT-3′; *Galectin-3*: Forward: 5′-CTTATTAACCTGCCTTTGCCTGG-3′, Reverse: 5′-GCAACATCATTCCCTCTTTGGA-3′; *GAPDH*: Forward: 5′-TGTGGGCATCAATGGATTTGG-3′, Reverse: 5′-ACACCATGTATTCCGGGTCAAT-3′. In addition, the relative gene expression was calculated using the $2^{-\Delta\Delta Ct}$ method, with *GAPDH* as the normalization control.

2.6 Cell Viability Assays

For the cell counting kit-8 (CCK-8) assay, the cells were seeded into 96-well plates and incubated at 37 °C. After 1, 2, 3, 4, 5, and 6 days, the cells were treated with CCK-8 reagent and incubated for 4 hours at 37 °C. OD value at 450 nm was measured using a Bio-Rad spectrophotometer (Berkeley, CA, USA).

For the 5-ethynyl-2′-deoxyuridine (EdU) assay, the cells were plated in 24-well plates and incubated at 37 °C for 24 hours. Subsequently, the cells were treated with EdU reagent (10 µM; RiboBio, Guangzhou, China) for 2 hours. Cells were then fixed with 4% paraformaldehyde, permeabilized with 0.5% Triton X-100, and stained with Apollo® reaction cocktail (RiboBio, China) according to the manufacturer's instructions. Nuclei were counterstained with DAPI (Sigma-Aldrich, Shanghai, China), and images were captured using a fluorescence microscope (Zeiss, Oberkochen, Germany).

2.7 Immunofluorescent Assays

BC cells were fixed with 4% paraformaldehyde (PFA) and blocked with 5% bovine serum albumin (BSA). Cells were then incubated with primary antibodies against CD41 (Abcam, ab134131; 1:200) and subsequently with secondary antibodies conjugated with Alexa 555 (Invitrogen, 1:1000, CA, USA) and phalloidin-FITC (Abcam, ab235137, 1:1000, UK). The nuclei were counterstained with DAPI for 5 minutes. Images were acquired using a fluorescence microscope (Zeiss, Germany).

2.8 Flow Cytometry (FCM) Assays

The MCF-7 cells were washed with PBS and fixed. They were then stained with anti-GPIb-IX (CD42b) antibody (BD Biosciences, Franklin Lake, NJ, USA, Cat# 551061, Lot# 123456) and anti-GP-IIb (CD41) antibody (BD Biosciences, Cat# 551061, Lot# 789012) for 20 minutes, and their expression levels were measured using a BD FACSCalibur (Franklin Lakes, NJ, USA) according to the manufacturer's instructions.

2.9 ELISA

The levels of T-box Protein 2 (TXB2) (Abcam, ab133054) and ATP production (Abcam, ab113849) in serum samples were measured using Enzyme-Linked Immunosorbent Assay (ELISA) kits (Abcam) following the manufacturer's guidelines.

2.10 Transwell-migration or Invasion Assays

Transwell inserts (BD Falcon) were used with 24-well plates as the lower chambers. For migration assays, the inserts were left uncoated. For invasion assays, inserts were coated with 100 µL of Matrigel (diluted 1:3 with serum-free media). Cells (1×10^5) were seeded in the upper chamber. After 24 hours, the cells that had migrated or invaded the underside of the membrane were fixed with 4% paraformaldehyde, stained with 0.2% crystal violet, and imaged.

2.11 Tube Formation Assay

HMEC cells were plated onto 24-well plates precoated with 50% Matrigel and cultured in medium from the MCF-7 cells upon the indicated transfections. Tube formation was assessed 4 hours later by capturing images with a fluorescence microscope (Carl Zeiss Inc, Oberkochen, Germany).

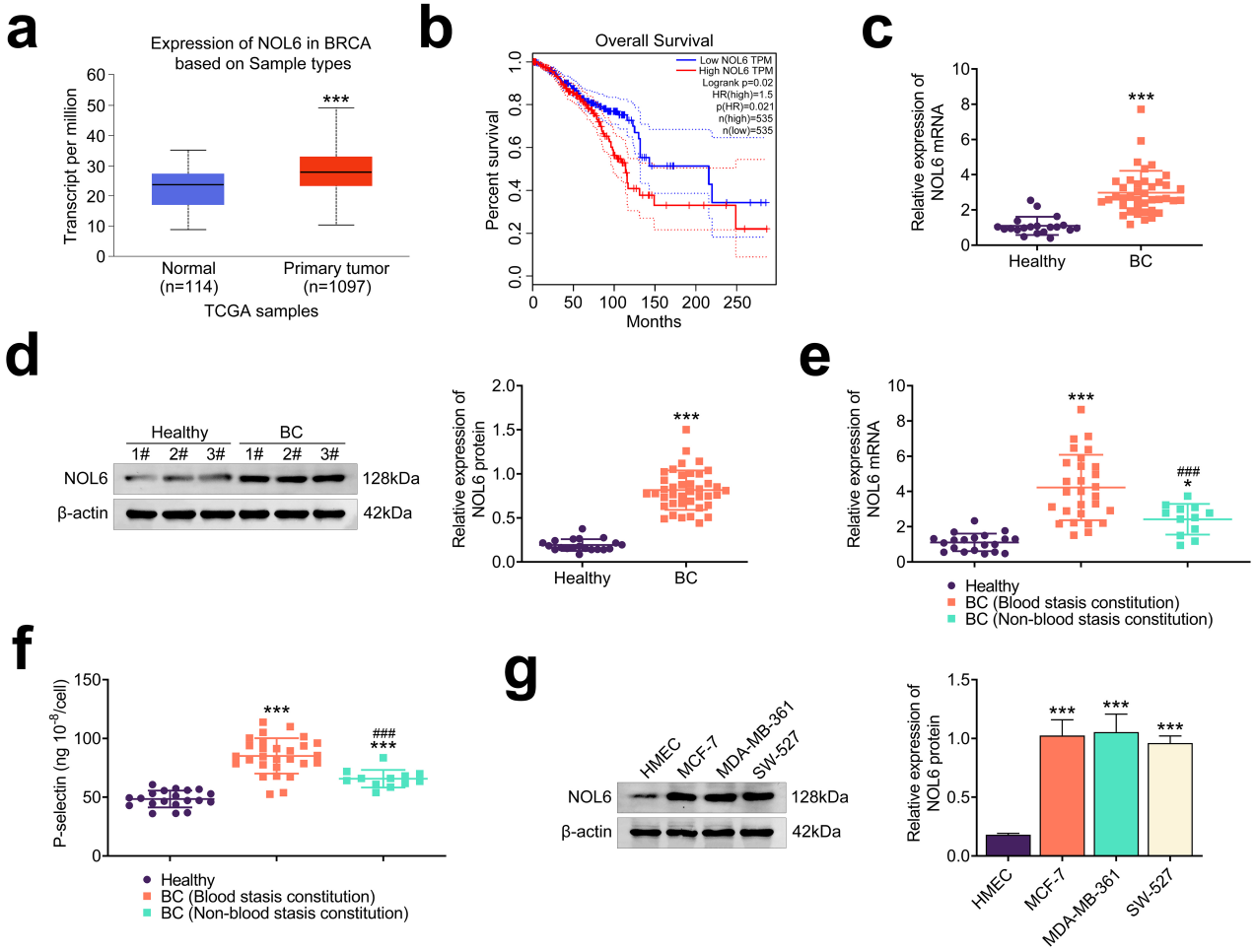

Fig. 1. NOL6 is highly expressed in BC. (a) TCGA database analysis of TPM values for NOL6 in 1097 tumor tissues and 114 normal tissues. ***$p < 0.001$. (b) Prognostic analysis from the GEPIA database showing overall survival rates based on NOL6 expression levels in BC patients ($p = 0.021$). (c) qPCR results demonstrating *NOL6* mRNA levels in tumor versus normal tissues. ***$p < 0.001$, BC vs healthy. (d) Immunoblot analysis of NOL6 expression in 3 representative BC tissues and 3 normal tissues (n = 3 per group). ***$p <$ 0.001, vs healthy. (e) qPCR data showing *NOL6* mRNA levels in serum from BC patients with blood stasis constitution versus those with non-blood stasis constitution (n = 40 per group). *$p < 0.05$, ***$p < 0.001$, vs healthy; ###$p < 0.001$ vs BC (blood stasis constitution). (f) P-selectin levels in serum from BC patients with blood stasis constitution compared to healthy controls. ***$p < 0.001$, vs healthy; ###p < 0.001 vs BC (blood stasis constitution). (g) Immunoblot demonstrating NOL6 expression in normal breast cell line HMEC and BC cell lines MCF-7, MDA-MB-231, and SW527. ***$p < 0.001$ vs HMEC. NOL6, GEPIA, Gene Expression Profiling Interactive Analysis; Nucleolar Protein 6; BC, Breast cancer; BRCA, Breast cancer; TCGA, The Cancer Genome Atlas; TPM, transcript per million; qPCR, quantitative PCR.

2.12 Tumor Growth in Vivo Assay

Nude mice (6-week-old female BALB/c nu/nu, purchased from Beijing Vital River Laboratory Animal Technology Co., Ltd., Beijing, China) were subcutaneously injected with 1×10^6 MCF-7 cells in 100 µL of PBS into the flanks. The mice were randomly divided into 2 groups (n = 6 per group): control shRNA, NOL6 shRNA. Tumor volume was measured every 4 days using calipers and calculated using the formula: volume = (length $\times$ width^2)/2. The tumor should not exceed 2000 mm^3 in mice. After 20 days, all mice were euthanized (cervical dislocation), and tumors were excised, weighed, and prepared for further analysis.

2.13 Immunohistochemical (IHC) Staining

Tissue samples were sliced, dehydrated through absolute alcohol, and rehydrated. The sections were fixed with 4% paraformaldehyde for 30 minutes, blocked with 2% BSA and then incubated with primary antibodies against CD41 (Abcam, ab134131; 1:200) and CD31 (Abcam, ab28364; 1:500) for 2 hours. All sections were incubated with HRP antibody for 1.5 h followed by adding diaminobenzidine in 5 min, and all sections were then counterstained with hematoxylin.

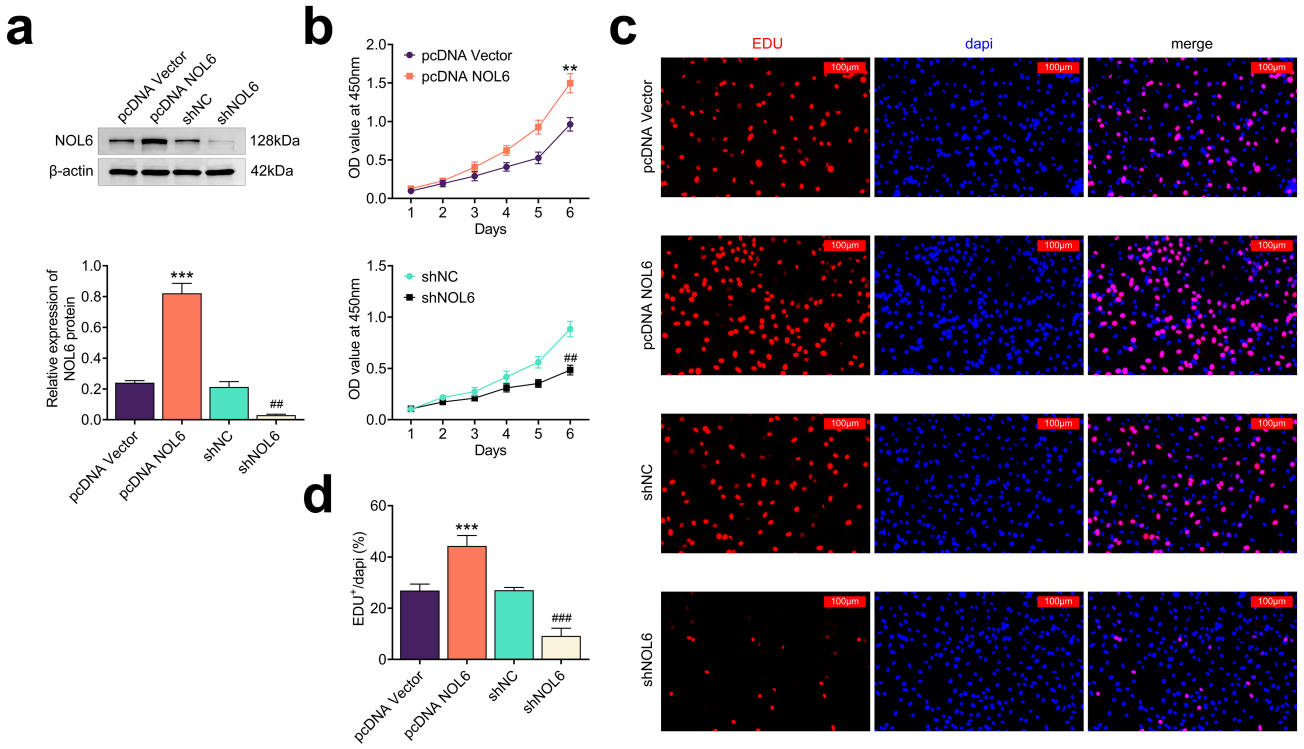

Fig. 2. Knockdown of NOL6 inhibits the growth of BC cells. (a) Immunoblot analysis showing NOL6 expression levels in MCF-7 cells following the indicated transfections. (b) CCK-8 assay results depicting the growth of MCF-7 cells with different NOL6 expression levels over 6 days, measured by OD450. (c) Edu assay images showing MCF-7 cell proliferation following the indicated transfections, with (d) quantification of Edu-positive cells per field. Scale bar, 100 μm. Each experiment was conducted in triplicate. $^{**}p < 0.01$, $^{***}p < 0.001$, pcDNA *NOL6* vs plasmid containing DNA (pcDNA) Vector; $\#\#p < 0.01$, $\#\#\#p < 0.001$, shNOL6 vs shNC. NC, negative control.

2.14 Statistical Analysis

Statistical analysis was performed using GraphPad 6.0 (GraphPad Software, Inc., Boston, MA, USA). For measurement data, the data were first assessed for normality using the Shapiro-Wilk test. For data that did not conform to a normal distribution, results are presented as medians with interquartile ranges, non-parametric tests were employed. Specifically, the Mann-Whitney U test was used to compare differences between two independent groups, and the Kruskal-Wallis test was applied for comparisons across multiple groups. Data are presented as mean ± SD for normally distributed data. Independent *t*-tests were used to compare the means between two groups. For categorical data, the data are presented as n (%). Statistical significance was determined using $p < 0.05$.

3. Results

3.1 NOL6 is Highly Expressed in BC

To investigate NOL6 expression in BC, we analyzed transcript per million (TPM) values from the TCGA database. The analysis revealed that NOL6 expression was significantly elevated in BC tissues compared to normal tissues ($p < 0.001$, Fig. 1a). Furthermore, the GEPIA database showed that high NOL6 expression was associated with poorer overall survival rates in BC patients ($p = 0.02$, Fig. 1b). To validate these findings, we conducted quantitative PCR (qPCR) assays and observed that NOL6 mRNA levels were significantly higher in tumor tissues than in normal tissues ($p < 0.001$, Fig. 1c). Consistent with these results, immunoblotting of representative BC tissues confirmed increased NOL6 expression ($p < 0.001$, Fig. 1d). Additionally, we examined *NOL6* mRNA levels in BC patients categorized by blood stasis constitution versus non-blood stasis constitution. The analysis showed that patients with a blood stasis constitution had higher NOL6 mRNA levels compared to those without this constitution ($p < 0.001$, Fig. 1e). Elevated P-selectin levels, which suggest increased platelet aggregation, were also observed in BC patients, particularly in those with blood stasis constitution ($p < 0.001$, Fig. 1f). This observation was supported by clinical pathological analysis, which indicated a correlation between NOL6 expression, P-selectin levels, blood coagulation function, and angiogenesis indicators, suggesting a link between NOL6 expression, platelet aggregation, and angiogenesis (Table 1). Furthermore, we assessed NOL6 expression in various BC cell lines, including MCF-7, MDA-MB-231, and SW527, and found sig-

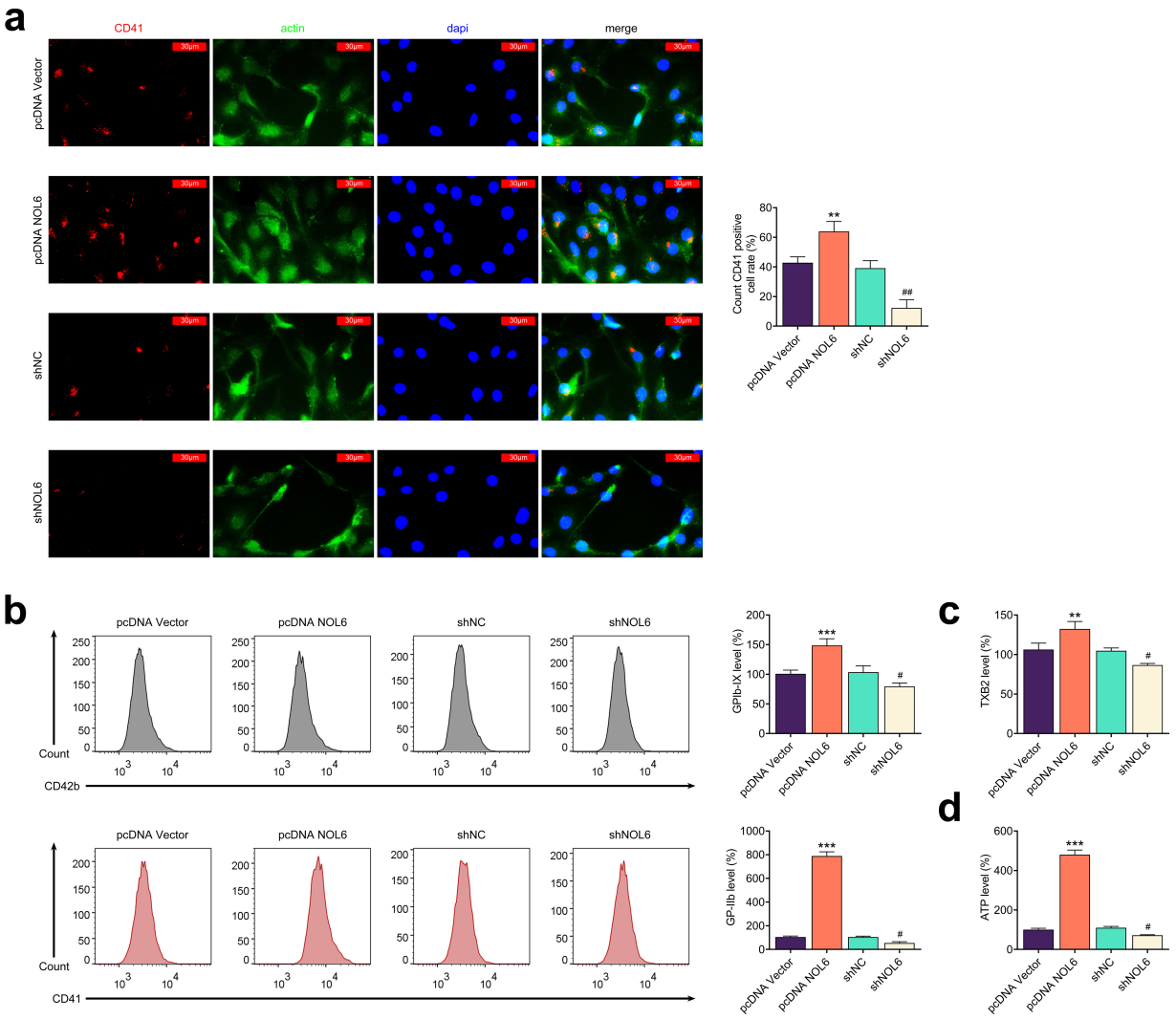

Fig. 3. Knockdown of NOL6 inhibits platelet aggregation induced by BC cells. (a) Immunostaining of CD41 in MCF-7 cells with the indicated transfections. Red panel indicates CD41, green panel indicates actin, and blue panel indicates DAPI. Scale bar, 30 μm. (b) Flow cytometry (FCM) analysis of GPIb-IX and GP-IIb expression levels in MCF-7 cells following different transfections. (c) Enzyme-Linked Immunosorbent Assay (ELISA) results showing TXB2 levels in MCF-7 cells with altered NOL6 expression. (d) Measurement of ATP levels in MCF-7 cells upon indicated transfections. Each experiment was conducted in triplicate. $**p < 0.01$, $***p < 0.001$, pcDNA NOL6 vs pcDNA Vector; $\#p < 0.05$, $\#\#p < 0.01$, shNOL6 vs shNC. NC, negative control. ELISA, Enzyme-Linked Immunosorbent Assay.

nificantly higher expression levels compared to the normal breast cell line HMEC ($p < 0.001$, Fig. 1g).

3.2 NOL6 Knockdown Inhibits BC Cell Growth

To elucidate the role of NOL6 in BC cell proliferation, we used shRNA and overexpression plasmids to modulate NOL6 expression in MCF-7 cells. We found that transfection with NOL6 overexpression plasmids resulted in a significant increase in NOL6 expression, while transfection with NOL6 shRNA plasmids led to a marked decrease in its expression ($p < 0.01$, Fig. 2a). Subsequent CCK-8 assays demonstrated that silencing NOL6 resulted in reduced viability of MCF-7 cells, whereas NOL6 overexpression significantly enhanced cell viability ($p < 0.01$, Fig. 2b). Similarly, Edu assays revealed that NOL6 knockdown impeded cell growth, as evidenced by a reduced percentage of Edu-positive cells, while NOL6 overexpression promoted an increase in Edu-positive cells ($p < 0.001$, Fig. 2c,d). These results collectively indicate that the knockdown of NOL6 effectively inhibits the growth of BC cells.

3.3 Knockdown of NOL6 Inhibits Platelet Aggregation Induced by BC Cells

Building on the observation that NOL6 promotes platelet aggregation in BC patients (Fig. 1f), we investigated how NOL6 influences platelet aggregation induced

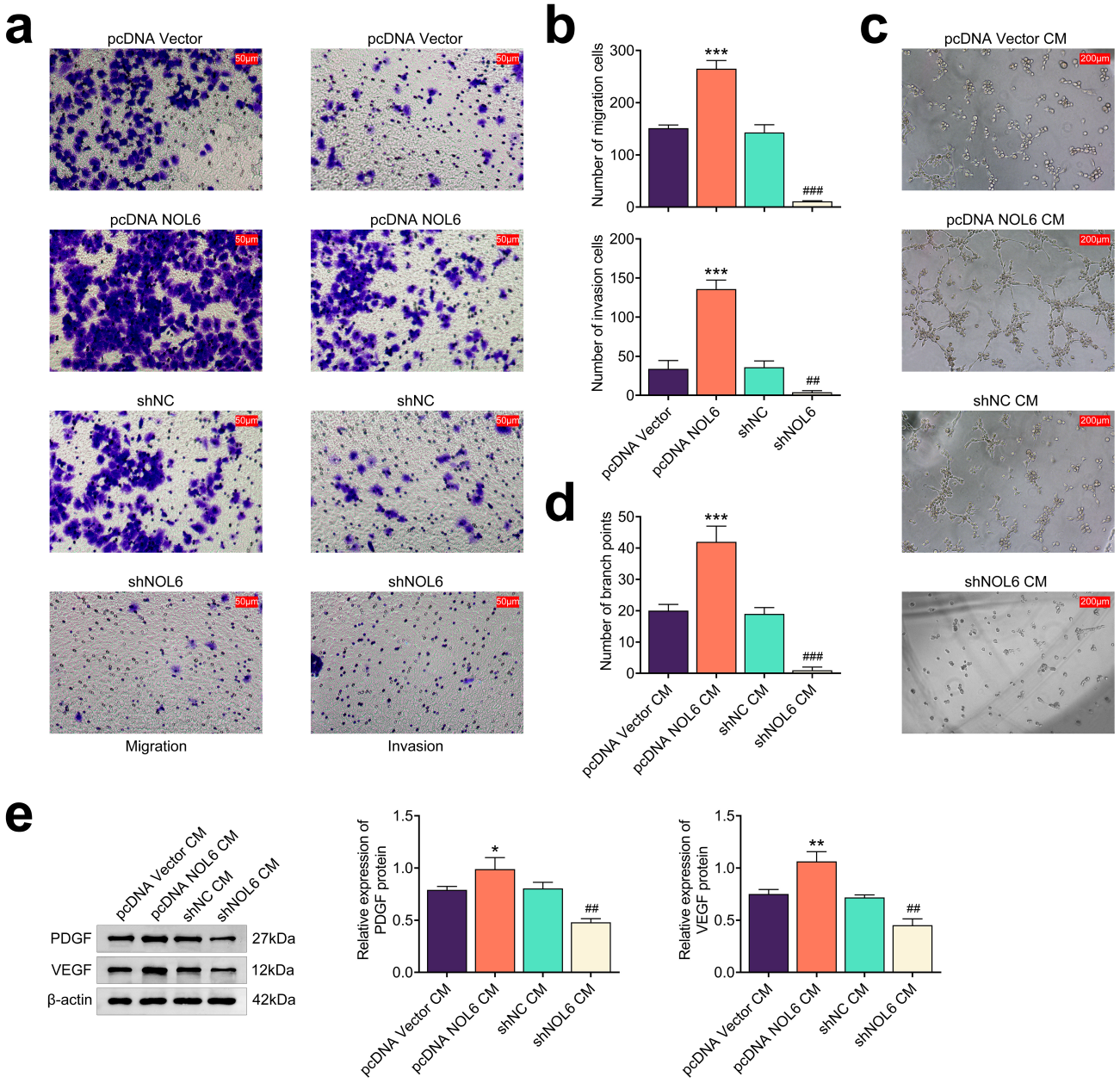

Fig. 4. Knockdown of NOL6 inhibits angiogenesis and motility of BC cells. (a) Transwell assays assessing the migration and invasion of MCF-7 cells following NOL6 modulation. Scale bar, 50 µm. (b) Quantification of migration and invasion cell counts from panel (a). (c) Tube formation assays illustrating the effects of NOL6 expression of MCF-7 cells and its culture medium on human umbilical vein endothelial cell (HUVEC) angiogenesis. Scale bar, 200 µm. CM, culture medium. (d) Quantification of branch points from panel (c). (e) Immunoblot analysis showing platelet-derived growth factor (PDGF) and vascular endothelial growth factor (VEGF) expression levels in HUVECs in response to NOL6 modulation in MCF-7 cells. Each experiment was conducted in triplicate. *$p < 0.05$, **$p < 0.01$, ***$p < 0.001$, pcDNA NOL6 vs pcDNA Vector; ##$p < 0.01$, ###$p < 0.001$, shNOL6 vs shNC. NC, negative control. HUVEC,Human Umbilical Vein Endothelial Cell. PDGF, platelet-derived growth factor; VEGF, Vascular endothelial growth factor.

by BC cells. Initially, MCF-7 cells were co-cultured with human platelets, and immunostaining assays were performed to assess the expression of the platelet aggregation marker CD41. The results showed that NOL6 overexpression in MCF-7 cells resulted in elevated CD41 levels ($p < 0.001$), whereas CD41 expression was significantly reduced in NOL6-depleted cells ($p < 0.01$, Fig. 3a). FCM assays further confirmed these findings by measuring the expression of GPIb-IX and GP-IIb, which are key markers of platelet aggregation. Overexpression of NOL6 led to increased levels of both GPIb-IX and GP-IIb ($p < 0.001$), while NOL6 knockdown reduced their expression, indicating a suppression of platelet aggregation ($p < 0.05$, Fig. 3b). In addition, enzyme-linked immunosorbent assays

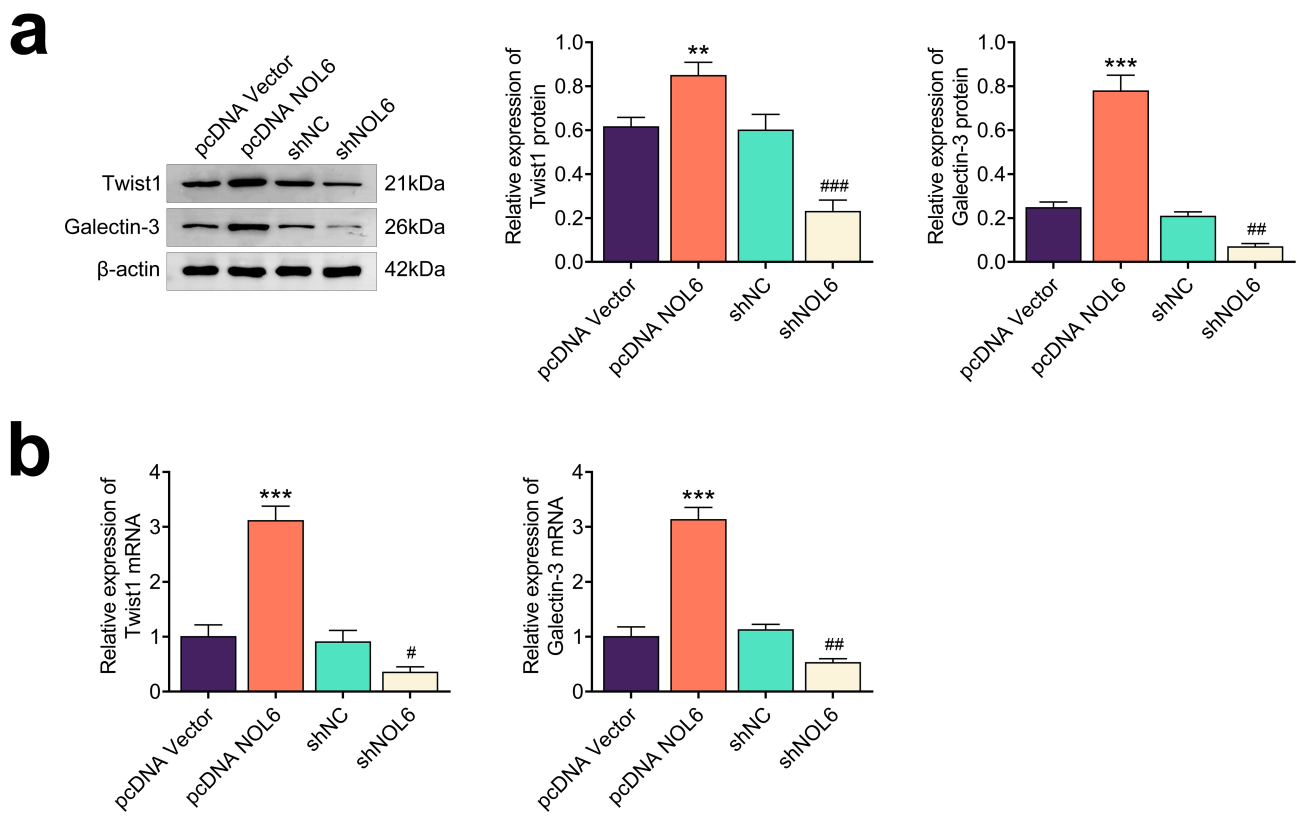

Fig. 5. NOL6 promotes the Twist1/galectin-3 axis in BC. (a) Immunoblot analysis of Twist1 and Galectin-3 expression in MCF-7 cells following NOL6 modulation. (b) qPCR assays assessing the mRNA levels of *Twist1* and *galectin-3* in MCF-7 cells upon NOL6 modulation. Each experiment was conducted in triplicate. $^{**}p < 0.01$, $^{***}p < 0.001$, pcDNA NOL6 vs pcDNA Vector; $\#p < 0.05$, $\#\#p < 0.01$, $\#\#\#p < 0.001$, shNOL6 vs shNC. NC, negative control.

(ELISA) demonstrated that the levels of TXB2, a marker associated with platelet aggregation, were higher in MCF-7 cells with NOL6 overexpression and lower in cells with NOL6 knockdown ($p < 0.01$), thus validating the role of NOL6 in platelet aggregation ($p < 0.05$, Fig. 3c). Moreover, ATP levels, which are indicative of platelet activation, were found to be increased in MCF-7 cells with NOL6 overexpression ($p < 0.001$) and decreased in cells with NOL6 knockdown ($p < 0.05$, Fig. 3d). Overall, these results indicate that the knockdown of NOL6 effectively inhibits platelet aggregation induced by BC cells.

3.4 Knockdown of NOL6 Inhibits Angiogenesis and Motility of BC Cells

To evaluate the impact of NOL6 on BC cell motility and angiogenesis, we performed several assays. Transwell assays revealed that NOL6 overexpression significantly enhanced the migration and invasion of MCF-7 cells ($p < 0.001$), while its depletion markedly reduced these processes ($p < 0.01$, Fig. 4a,b). Subsequent tube formation assays demonstrated that NOL6 overexpression in MCF-7 cells increased the angiogenic potential of HMECs, as evidenced by a higher number of branch points ($p < 0.001$, Fig. 4c,d). In contrast, NOL6 depletion led to a significant reduction in angiogenesis by Human Umbilical Vein Endothelial Cells (HUVECs) ($p < 0.001$, Fig. 4c,d). Additionally, immunoblotting analysis showed that NOL6 overexpression upregulated the expression of angiogenesis-related factors, such as PDGF and VEGF ($p < 0.05$), whereas NOL6 depletion resulted in decreased levels of these factors ($p < 0.01$, Fig. 4e). Taken together, these findings collectively indicate that the knockdown of NOL6 inhibits both the angiogenic capacity and motility of BC cells.

3.5 NOL6 Promotes the Twist1/galectin-3 Axis in BC

Next, we explored the underlying mechanism by which NOL6 influences BC through immunoblot analyses. We observed that overexpression of NOL6 resulted in increased levels of Twist1 and galectin-3 in MCF-7 cells, while NOL6 depletion led to reduced expression of these proteins, suggesting a regulatory role of NOL6 in the Twist1/galectin-3 axis ($p < 0.01$, Fig. 5a). This observation was further supported by qPCR assays, which confirmed that NOL6 modulates the mRNA levels of *Twist1* and *galectin-3* in MCF-7 cells ($p < 0.01$, Fig. 5b).

Additionally, we investigated whether the effects of NOL6 depletion could be reversed by Twist1 overexpression. The results from both immunoblot and qPCR assays

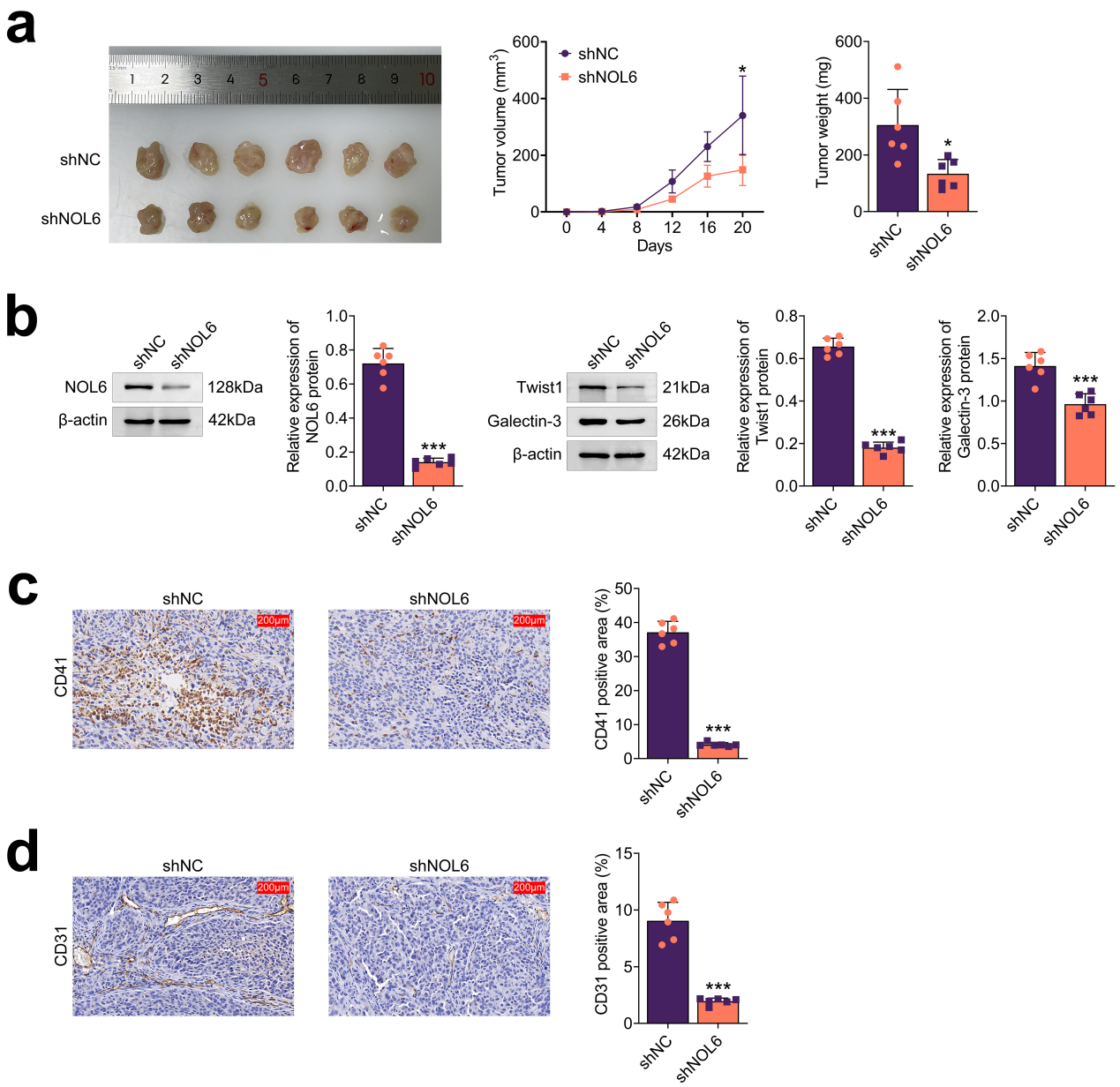

Fig. 6. NOL6 inhibits the growth of BC *in vivo*. (a) Tumor growth assays illustrating the effects of NOL6 on BC progression *in vivo*. Representative images of tumors are shown (left), with tumor volume and weight measured every 4 days over 20 days (n = 6 per group). (b) Immunoblot analysis displaying the expression of NOL6 (left), Twist1, and Galectin-3 (right) in tumor tissues from the indicated groups. (c) Immunohistochemical (IHC) assays showing CD41 expression in tumor tissues, with quantitative analysis included. Scale bar, 200 μm. (d) IHC assays showing CD31 expression in tumor tissues, with quantitative analysis included. Scale bar, 200 μm. Each experiment was performed in triplicate. *$p < 0.05$, ***$p < 0.001$, shNOL6 vs shNC. NC, negative control. IHC, Immunohistochemical.

demonstrated that Twist1 overexpression rescued the expression levels of Twist1 and galectin-3 reduced by NOL6 depletion ($p < 0.01$, **Supplementary Fig. 1a,b**). Furthermore, CCK-8 assays showed that Twist1 overexpression mitigated the inhibition of MCF-7 cell growth induced by NOL6 depletion ($p < 0.001$, **Supplementary Fig. 1c**). Flow cytometry (FCM) assays revealed that Twist1 overexpression restored the levels of GPIb-IX and GP-IIb in MCF-7 cells following NOL6 depletion, suggesting a recovery in platelet aggregation potential ($p < 0.01$, **Supplementary Fig. 1d**). Similarly, ELISA showed that Twist1 overexpression counteracted the decrease in TXB2 levels caused by NOL6 ablation ($p < 0.01$, **Supplementary Fig. 1e**). Finally, Twist1 overexpression reversed the suppression of tube formation in MCF-7 cells induced by NOL6 depletion, as observed in tube formation assays ($p < 0.001$, **Supplementary Fig. 1f**). In summary, these results collectively demonstrate that NOL6 promotes the Twist1/galectin-3 axis in BC, influencing both cellular growth and platelet aggregation.

3.6 NOL6 Inhibits the Growth of BC in Vivo

To assess the impact of NOL6 on BC tumor growth *in vivo*, we utilized shRNAs targeting NOL6 to decrease its expression in MCF-7 cells. These NOL6-depleted MCF-7 cells were then injected subcutaneously into the abdomen of nude mice. After 20 days, the results demonstrated that NOL6 ablation led to a significant suppression of tumor growth, as evidenced by reduced tumor volume and weight ($p < 0.05$, Fig. 6a). The silencing efficiency of NOL6 in the tumors was confirmed by immunoblot analysis, which also showed decreased levels of Twist1 and galectin-3 in the tumor tissues from NOL6-depleted mice ($p < 0.001$, Fig. 6b). Immunohistochemical (IHC) assays further revealed that NOL6 depletion resulted in reduced CD41 levels in tumor tissues, indicating suppression of platelet aggregation ($p < 0.001$, Fig. 6c). Additionally, a decrease in CD31 levels was observed in the tumor tissues from NOL6-depleted mice, suggesting an inhibition of angiogenesis ($p < 0.001$, Fig. 6d). These findings collectively suggest that NOL6 plays a role in promoting BC tumor growth *in vivo*, and its depletion leads to reduced tumor progression through mechanisms involving platelet aggregation and angiogenesis.

4. Discussion

BC treatment typically involves a comprehensive approach tailored to individual patient profiles [12]. While targeted therapy represents a promising strategy for advanced BC, further research into the underlying mechanisms and the development of novel therapeutic targets is crucial. Notably, abnormal coagulation indices in BC patients suggest a dysregulation in coagulation, which may contribute to tumor progression and metastasis [13]. Platelets play a significant role in the survival and dissemination of tumor cells. The interaction between circulating tumor cells and platelets promotes metastasis through physical contact and bidirectional activation [14]. Tumor cell-induced platelet aggregation (TCIPA) facilitates immune evasion and enhances tumor cell adhesion and invasion [15]. Additionally, tumor-induced platelets release soluble mediators that increase tumor cell invasiveness and bone metastasis in animal models [16,17]. In this present study, our findings indicate that NOL6 knockdown inhibits platelet aggregation induced by BC cells, thereby suppressing both tumor progression and metastasis.

Angiogenesis plays an essential role in BC development. This complex biological process involves various molecules, including cytokines, growth factors, receptor proteins, cell membrane molecules, transcription factors, and signaling pathway molecules [18]. Understanding the roles and interactions of these molecules is essential for gaining insights into the biological characteristics of BC angiogenesis. Such knowledge can offer new approaches and strategies for BC treatment. Endothelial cell growth and directional migration are critical aspects of angiogenesis [19]. In this study, we demonstrate that the ablation of NOL6 impairs both angiogenesis and the migration of BC cells.

NOL6 is a nucleolar protein that has been highly conserved throughout evolution. It is closely associated with chromosome condensation during mitosis. Additionally, NOL6/NRAP protein stress has been reported to activate p53/CP-1-mediated immune mechanisms, thereby influencing tumor progression [6]. It has been shown that NOL6 plays an important role in cell cycle maintenance and tumor cell invasiveness. Investigating the relationship and mechanisms between NOL6 expression and BC is crucial for developing effective treatment strategies [5]. Our data confirm the high expression of NOL6 in BC, which contributes to various processes, including platelet aggregation and angiogenesis, which facilitate BC progression.

Galectin-3, a multifunctional proto-oncoprotein, plays a significant role in regulating tumor cell growth, invasion, angiogenesis, and apoptosis. It has potential as a novel diagnostic marker for tumor metastasis and is a candidate for targeted cancer therapies [20]. Additionally, Twist1, an upregulated marker in dormant BC cells [9,21], is closely associated with invasion, metastasis, prognosis, drug resistance, and angiogenesis in BC [22]. Twist1 enhances the expression of the proto-oncogene AKT2 by binding to its promoter, which in turn activates YB-1, a protein involved in cell growth, thus promoting tumor cell proliferation [23]. Our findings indicate that NOL6 influences platelet aggregation, angiogenesis, motility, and tumor growth in BC through the Twist1/galectin-3 axis.

5. Conclusions

In conclusion, our study demonstrates that NOL6 is highly expressed in BC and facilitates platelet aggregation and angiogenesis through the Twist1/galectin-3 axis, supporting NOL6 as a potential therapeutic target in BC.

Availability of Data and Materials

The datasets used and/or analyzed during the present study are available from the corresponding author on reasonable request.

Author Contributions

TZ, CL, ML, SD and XW contributed to the study conception and design. Material preparation and the experiments were performed by TZ. Data collection and analysis were performed by CL, ML and SD. The first draft of the manuscript was written by XW and all authors commented on previous versions of the manuscript. All authors read and approved the final manuscript. All authors contributed to editorial changes in the manuscript. All authors have participated sufficiently in the work and agreed to be accountable for all aspects of the work.

Ethics Approval and Consent to Participate

The serum samples study has been approved by the Ethics Committee of the Lianyungang Affiliated Hospital of Nanjing University of Chinese Medicine (Approval No.: 2023-13). Written informed consent was obtained from legally authorized representative(s) for anonymized patient information to be published in this article. This study was conducted in accordance with the principles outlined in the Declaration of Helsinki. All animal experiments were approved by the Ethics Committee of Lianyungang Affiliated Hospital of Nanjing University of Traditional Chinese Medicine for the use of animals and conducted in accordance with the National Institutes of Health Laboratory Animal Care and Use Guidelines.

Acknowledgment

Not applicable.

Funding

This work was supported by the present study was financially supported by the Natural Science Foundation of Jiangsu Province (Grant No. BK20211018) and Science and Technology project of Lianyungang Administration of Traditional Chinese Medicine (Grant No. LZYYB202306).

Conflict of Interest

The authors declare no conflict of interest.

Supplementary Material

Supplementary material associated with this article can be found, in the online version, at https://doi.org/10.31083/FBL25361.

References

[1] Zhang L, Qiang J, Yang X, Wang D, Rehman AU, He X, *et al*. IL1R2 Blockade Suppresses Breast Tumorigenesis and Progression by Impairing USP15-Dependent BMI1 Stability. Advanced Science (Weinheim, Baden-Wurttemberg, Germany). 2019; 7: 1901728. https://doi.org/10.1002/advs.201901728.

[2] Xia X, Huang C, Liao Y, Liu Y, He J, Shao Z, *et al*. The deubiquitinating enzyme USP15 stabilizes ERα and promotes breast cancer progression. Cell Death & Disease. 2021; 12: 329. https://doi.org/10.1038/s41419-021-03607-w.

[3] Sun X, Tang H, Chen Y, Chen Z, Hu Z, Cui Z, *et al*. Loss of the receptors ER, PR and HER2 promotes USP15-dependent stabilization of PARP1 in triple-negative breast cancer. Nature Cancer. 2023; 4: 716–733. https://doi.org/10.1038/s43018-023-00535-w.

[4] Lian L, Li W, Li ZY, Mao YX, Zhang YT, Zhao YM, *et al*. Inhibition of MCF-7 breast cancer cell-induced platelet aggregation using a combination of antiplatelet drugs. Oncology Letters. 2013; 5: 675–680. https://doi.org/10.3892/ol.2012.1074.

[5] Dong D, Song M, Wu X, Wang W. NOL6, a new founding oncogene in human prostate cancer and targeted by miR-590-3p. Cytotechnology. 2020; 72: 469–478. https://doi.org/10.1007/s10616-020-00394-8.

[6] He L, Qian X, Ge P, Fan D, Ma X, Wu Q, *et al*. NOL6 Regulates the Proliferation and Apoptosis of Gastric Cancer Cells *via* Regulating TP53I3, CDK4 and MCM7 Expression. Frontiers in Oncology. 2022; 12: 708081. https://doi.org/10.3389/fonc.2022.708081.

[7] Liang J, Sun W, Song H, Wang C, Li Q, Li C, *et al*. NOL6 promotes the proliferation and migration of endometrial cancer cells by regulating *TWIST1* expression. Epigenomics. 2021; 13: 1571–1585. https://doi.org/10.2217/epi-2021-0218.

[8] Mohammed Zaidh S, Aher KB, Bhavar GB, Irfan N, Ahmed HN, Ismail Y. Genes adaptability and NOL6 protein inhibition studies of fabricated flavan-3-ols lead skeleton intended to treat breast carcinoma. International Journal of Biological Macromolecules. 2024; 258: 127661. https://doi.org/10.1016/j.ijbiomac.2023.127661.

[9] Wu H, Li A, Zheng Q, Gu J, Zhou W. LncRNA LZTS1-AS1 induces proliferation, metastasis and inhibits autophagy of pancreatic cancer cells through the miR-532 /TWIST1 signaling pathway. Cancer Cell International. 2023; 23: 130. https://doi.org/10.1186/s12935-023-02979-7.

[10] Abdulaziz A. Deregulation of TWIST1 expression by promoter methylation in gastrointestinal cancers. Saudi Journal of Biological Sciences. 2024; 31: 103842. https://doi.org/10.1016/j.sjbs.2023.103842.

[11] Cui H, Hou C, Ma Q, Chen Z, Xie X. Effect and Mechanism of lncRNA-PCMF1/hsa-miR-137/Twist1 Axis Involved in the EMT Regulation of Prostate Cancer Cells. Molecular Biotechnology. 2023; 65: 1991–2003. https://doi.org/10.1007/s12033-023-00709-y.

[12] Nandi SK, Chatterjee N, Roychowdhury T, Pradhan A, Moiz S, Manna K, *et al*. Kaempferol with Verapamil impeded panoramic chemoevasion pathways in breast cancer through ROS overproduction and disruption of lysosomal biogenesis. Phytomedicine: International Journal of Phytotherapy and Phytopharmacology. 2023; 113: 154689. https://doi.org/10.1016/j.phymed.2023.154689.

[13] Cao J, Ma X, Yan X, Zhang G, Hong S, Ma R, *et al*. Kaempferol induces mitochondrial dysfunction and mitophagy by activating the LKB1/AMPK/MFF pathway in breast precancerous lesions. Phytotherapy Research: PTR. 2023; 37: 3602–3616. https://doi.org/10.1002/ptr.7838.

[14] Afzal M, Alarifi A, Karami AM, Ayub R, Abduh NAY, Saeed WS, *et al*. Antiproliferative Mechanisms of a Polyphenolic Combination of Kaempferol and Fisetin in Triple-Negative Breast Cancer Cells. International Journal of Molecular Sciences. 2023; 24: 6393. https://doi.org/10.3390/ijms24076393.

[15] Wang Y, Zhang C, Mai L, Niu Y, Wang Y, Bu Y. PRR11 and SKA2 gene pair is overexpressed and regulated by p53 in breast cancer. BMB Reports. 2019; 52: 157–162. https://doi.org/10.5483/BMBRep.2019.52.2.207.

[16] Pooladanda V, Bandi S, Mondi SR, Gottumukkala KM, Godugu C. Nimbolide epigenetically regulates autophagy and apoptosis in breast cancer. Toxicology in Vitro: an International Journal Published in Association with BIBRA. 2018; 51: 114–128. https://doi.org/10.1016/j.tiv.2018.05.010.

[17] Li T, Zhou Y, Li D, Zeng Z, Zhang S. The role of genome-scale leukocyte long noncoding RNA in identifying acute aortic dissection. Signa Vitae. 2022; 18: 101–110.

[18] Dong ZX, Chan SH, Chen SN, Li M, Zhang XD, Liu XQ. TJP1 promotes vascular mimicry in bladder cancer by facilitating VEGFA expression and transcriptional activity through TWIST1. Translational Oncology. 2023; 32: 101666. https://doi.org/10.1016/j.tranon.2023.101666.

[19] Jia H, Thelwell C, Dilger P, Bird C, Daniels S, Wadhwa M. Endothelial cell functions impaired by interferon in vitro: Insights into the molecular mechanism of thrombotic microangiopathy

associated with interferon therapy. Thrombosis Research. 2018; 163: 105–116. https://doi.org/10.1016/j.thromres.2018.01.039.

[20] Barut Z, Nalbantoğlu AM, Korkmaz H, Demir Z, Hatipoğlu M, Özkan A, *et al*. The role of salivary galectin-3 and galectin-9 levels in plaque-induced gingivitis and periodontitis. Heliyon. 2023; 9: e19979. https://doi.org/10.1016/j.heliyon.2023.e19979.

[21] Lee S, Kang E, Lee U, Cho S. Role of pelitinib in the regulation of migration and invasion of hepatocellular carcinoma cells via inhibition of Twist1. BMC Cancer. 2023; 23: 703. https://doi.org/10.1186/s12885-023-11217-2.

[22] Liu Y, Chen M, Wu B. TWIST1 Promotes Colorectal Carcinoma Stemness and Oxaliplatin Resistance by Activating Microfibrillar-Associated Protein 2. Assay and Drug Development Technologies. 2023; 21: 202–211. https://doi.org/10.1089/adt.2022.099.

[23] Gong A, Wang X, Wang X, Zhao Y, Cui Y. Twist1 Promoter Methylation Regulates the Proliferation and Apoptosis of Acute Myeloid Leukemia Cells via PI3K/AKT Pathway. Indian Journal of Hematology & Blood Transfusion: an Official Journal of Indian Society of Hematology and Blood Transfusion. 2023; 39: 25–32. https://doi.org/10.1007/s12288-022-01540-2.